Geomechanics and Engineering, *Vol. 29, No. 4 (2022) 451-461*
https://doi.org/10.12989/gae.2022.29.4.451

Dynamic response of coal and rocks under high strain rate

Jingxuan Zhou[1,2], Chuanjie Zhu*[1], Jie Ren[1], Ximiao Lu[1], Cong Ma[1] and Ziye Li[1]

[1]*Faculty of Safety Engineering, China University of Mining and Technology, Xuzhou, Jiangsu, 221116, China*
[2]*Department of Structural Engineering, Tongji University, Shanghai, 200092, China*

(Received April 5, 2020, Revised March 22, 2022, Accepted April 3, 2022)

Abstract. The roadways surrounded by rock and coal will lose their stability or even collapse under rock burst. Rock burst mainly involves an evolution of dynamic loading which behaves quite differently from static or quasi-static loading. To compare the dynamic response of coal and rocks with different static strengths, three different rocks and bituminous coal were selected for testing at three different dynamic loadings. It's found that the dynamic compression strength of rocks and bituminous coal is much greater than the static compression strength. The dynamic compression strength and dynamic increase factor of the rocks both increase linearly with the increase of the strain rate, while those of the bituminous coal are irregular due to the characteristics of multi-fracture and heterogeneity. Moreover, the absorbed energy of the rocks and bituminous coal both increase linearly with an increase in the strain rate. And the ratio of absorbed energy to the total energy of bituminous coal is greater than that of rocks. With the increase of dynamic loading, the failure degree of the sample increases, with the increase of the static compressive strength, the damage degree also increases. The static compassion strength of the bituminous coal is lower than that of rocks, so the number of small-scale fragments was the largest after bituminous coal rupture.

Keywords: compression strength; dynamic loading; SHPB; strain rate; stress-strain

1. Introduction

In-situ stress of rock formation is increasing with the increase of coal mining depth (Bieniawski 1968, Brown and Hoek 1978). The in-situ stress will redistribute due to coal mining (Read 2004, Cai 2008), which leads to stress concentration and non-negligible rock burst (a kind of dynamic disaster frequently occurred in underground coal mines) (Wang and Park 2001, He *et al*. 2015). The rock burst causes sudden collapse of the surrounding rock, which will induce instability and even failure of coal mine roadways, whose vibration may even endanger the ground buildings.

Previous scholars have conducted extensive research on the mechanical response and static mechanical properties of roadway surrounding rock under in-situ stress (Li *et al.* 2012, Yaméogo *et al.* 2013, Meng *et al.* 2016). The surrounding rock of deep roadway has experienced a long process, contains a lot of energy, and is prone to rock burst, which has a short duration and huge harm. Transient loading plays a major role in rock burst. The rock burst mainly involves an evolution of dynamic loading which behaves quite differently from static or quasi-static loading (Field *et al.* 2004). (Abrams 1917) found that the dynamic strength of concrete was larger than its static strength in 1917. (Wang *et al.* 2006) furtherly demonstrated that the dynamic strength and elastic modulus of rocks were several times higher than of the static ones by the dynamic tensile test. Previous scholars have done plenty of research on the dynamic properties of rock, and there are a variety of research methods and conclusions. In recent years, many scholars have studied the dynamic mechanical properties of rock through experiments (Wla *et al*. 2012, Tao *et al.* 2017) and numerical simulation (Yilmaz and Unlu 2013).

A commonly used dynamic loading test technique is the Split-Hopkinson Bar Material Tests (SHPB) (Davies and Hunter 1963, Gama *et al*. 2004, Crespo *et al.* 2017). Many researchers have used it to study the dynamic response of different kinds of materials and found that the dynamic strength and rupture degree of rocks are related to dynamic loading rate and strain rate (Feng *et al.* 2016, Yao *et al.* 2017, Kim *et al*. 2018, Li *et al*. 2018, Chen *et al*. 2019). Strain rate can be classified according to its amplitude: low strain rates (10^{-5}-10^{-2} s^{-1}), intermediate strain rates (10^{-2}-10^{2} s^{-1}), high strain rates (10^{2}-10^{4} s^{-1}), and ultrahigh strain rates (more than 10^{4} s^{-1}) (Blanton 1981, Tarasov 1990, Liu and Xu 2015). Most results show that there are linear or other forms of relationship between dynamic mechanical properties and strain rates (Cho *et al*. 2003, Li *et al.* 2005, Demirdag *et al.* 2010). Wang found that the energy utilization rate decreased with the increase of dynamic impact load (Wang *et al*. 2019). Using the combination of numerical simulation and SHPB, Zhu found that the failure of rock under dynamic-static coupling is related to its heterogeneity (Zhu *et al.* 2016).

Most of the previous research focused on the same kind of rock, while the dynamic mechanical properties of coal (a kind of porous rock with very low strength) were rarely studied. And the comparative analysis of rocks and coal is more limited. The surrounding rock of the coal mine roadway is composed of different coals and rocks. Due to the non-uniformity and low strength characteristics of coal

*Corresponding author, Professor
E-mail: anq021@126.com

ISSN: 2005-307X (Print), 2092-6219 (Online)

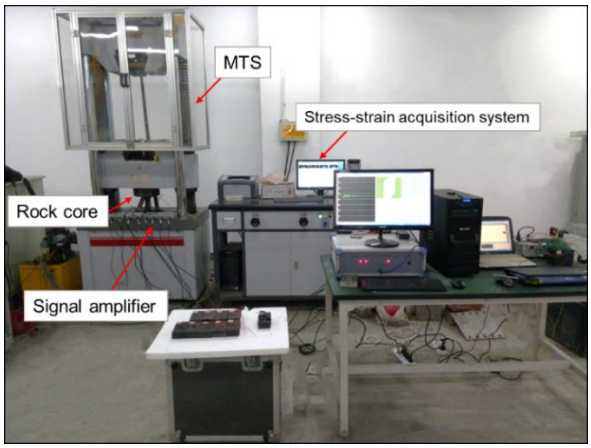

Fig. 1 Schematic diagram of the experiment system

(Liu *et al.* 2004, Liu *et al*. 2017), its dynamic response is very different from that of rocks. Therefore, it is necessary to analyze rocks and coals. In the present work, the strength of rocks and coal was determined by static mechanical experiments. The purpose of the study was to ascertain the effect of rock strength on its dynamic mechanical properties at different strain rates and to compare these with coal.

2. Experiments

2.1 Sample preparation

Three kinds of rocks with different static strength and bituminous coal were selected in our experiments, e.g., limestone, sandstone, and shale. Cylindrical rock and coal cores were used in our tests and were cut from a large rock and coal blocks. The diameter of the rocks used in the static mechanical property test was 50 mm with a height of 100 mm. It was 100 mm and 50 mm, respectively, in the dynamic mechanical property test.

2.2 Experiment system

(1) Static mechanical property test system

The static stress-strain curves of the rocks and coal cores were tested by a uniaxial compression experiment system (shown in Fig. 1). The system mainly includes a compression loading system (MTS C64.605, MTS Industrial System CO.LTD), a stress-strain acquisition system, and other accessories. The loading rate of the MTS system is 0.1 mm/min in our experiments. The stress-strain evolution of the rocks was monitored by the stress-strain acquisition system (DH3817, Tonghua Testing Technology Co. LTD, China).

(2) Dynamic mechanical property test system

Fig.2 shows the Split Hopkinson Pressure Bar (SHPB) used in the test of the dynamic mechanical properties of the rocks. The SHPB includes a pressure bar system (including a high-pressure nitrogen bottle, an air chamber, a launch cavity, a striker bar, an incident bar, a transmission bar, and an adsorption bar), air pressure controller, speed measuring system (including speed measuring circuit and time interval instrument), strain collection system (including two strain gauges and transient waveform storage instrument) and data processing system. All bars have the same cross-section diameter of 100 mm. The length of the striker bar and the transmission bar with an elastic modulus of 210 GPa is 2 m. During the tests, the striker bar impacts the free end of the incident bar and produces a longitudinal compression wave (incident wave) in the incident bar. When the compression wave arrives at the interface between the incident bar and rock cores, it is partly reflected (reflected wave) and the rest passes through the rock cores into the transmission bar (transmitted wave). In this test, the impact air pressure of 0.05 MPa, 0.06 MPa, and 0.08 MPa was used to control the impact velocity of the bullet. Based on the assumption of one-dimensional stress wave and stress homogenization (Kolsky 1954), the dynamic response parameters of the rock cores can be calculated by Eqs. (1)-(3) (Frew *et al.* 2001, Yavuz *et al*. 2013, Liu *et al.* 2019).

$$\dot{\varepsilon}(t) = \frac{C_0}{L_0}[\varepsilon_i(t) - \varepsilon_r(t) - \varepsilon_t(t)] \tag{1}$$

$$\varepsilon(t) = \frac{C_0}{L_0}\int_0^t [\varepsilon_i(t) - \varepsilon_r(t) - \varepsilon_t(t)]dt \tag{2}$$

$$\sigma = \frac{A}{2A_0}E[\varepsilon_i(t) + \varepsilon_r(t) + \varepsilon_t(t)] \tag{3}$$

Where, ε, $\dot{\varepsilon}$, and σ is strain, strain rate and stress of the rock cores; ε_i, ε_r, and ε_t is the incident, reflected and transmitted strain, respectively; C_0, L_0, and E is wave velocity of elastic wave, length of the rock cores and elastic modulus of the bar, respectively. A and A_0 is the cross-section area of the bar and rock cores, respectively.

According to the assumption of stress homogenization of rock cores, it can also be obtained that

$$\varepsilon_t(t) = \varepsilon_i(t) + \varepsilon_r(t) \tag{4}$$

Then, formula (1), (2) and (3) can be converted to

$$\dot{\varepsilon}(t) = \frac{-2C_0}{L_0}\varepsilon_r(t) \tag{5}$$

$$\varepsilon(t) = \frac{-2C_0}{L_0}\int_0^t \varepsilon_r(t)dt \tag{6}$$

$$\sigma(t) = \frac{AE}{A_0}\varepsilon_t(t) \tag{7}$$

3. Results and discussion

3.1 Static mechanical properties

Static mechanical parameters of the four kinds of samples (limestone, sandstone, shale, and bituminous coal) were given in Table 1. Each value is an average one from three separate tests. As shown in Table 1, the static compression strength of shale is highest and that of the bituminous coal is the lowest.

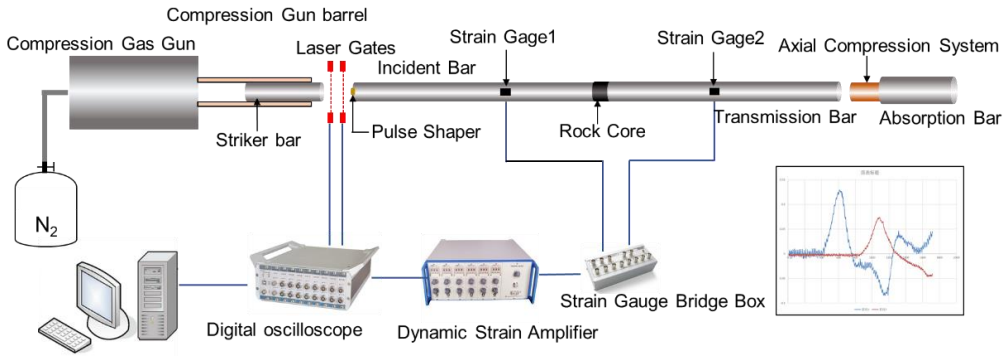

Fig.2 Dynamic mechanical properties test system

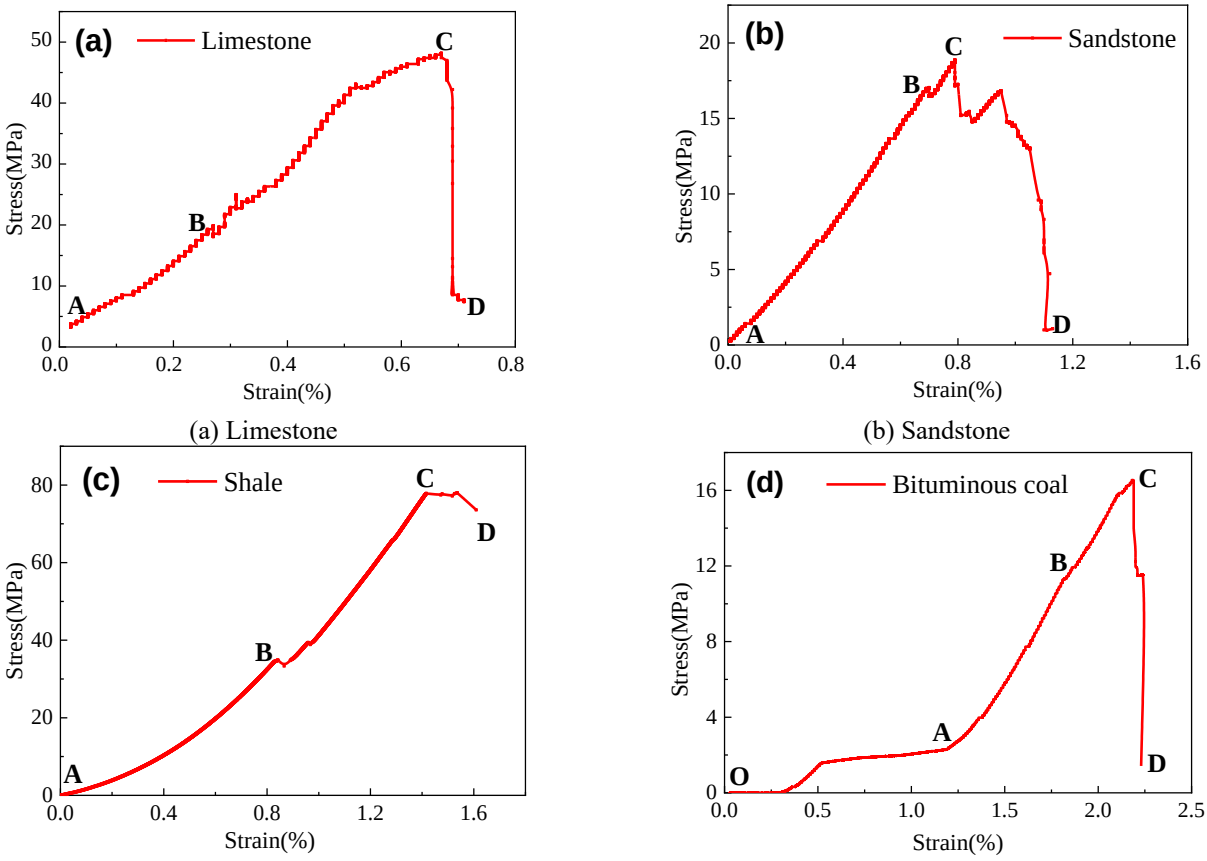

(a) Limestone (b) Sandstone

(c) Shale (d) Bituminous coal

Fig. 3 Stress-strain curves of rock cores in static mechanical property test

Table 1 Static mechanical parameters of rocks and coal

Rock types	Density /g/cm^3	Static compression strength /MPa	Elastic modulus /GPa	Poisson's ratio
Limestone	2.478	48.33	38.37	0.26
Sandstone	2.333	20.05	24.68	0.20
Shale	2.516	77.98	30.59	0.24
Bituminous coal	1.296	15.96	8.29	0.32

Fig. 3 shows stress-strain curves of the three kinds of rocks and the bituminous coal under static compression loading. Compression failure process of the rocks and coal can be divided into four stages: pore compaction stage, elastic stage, plastic stage, and post-peak failure stage.

(1) Pore compaction stage (OA). For the bituminous coal, when the compression loading kept increasing, the micro-cracks and pores were compacted and new cracks had not yet developed, during which the stress was maintained at a nearly constant value while the strain increased dramatically. However, there was no obvious pore compaction stage for rocks.

(2) Elastic deformation stage (AB). The stress and strain increased linearly under the compression loading. The elastic modulus of the limestone, sandstone, and shale is 38.37 GPa, 24.68 GPa, and 30.59 GPa, respectively, which

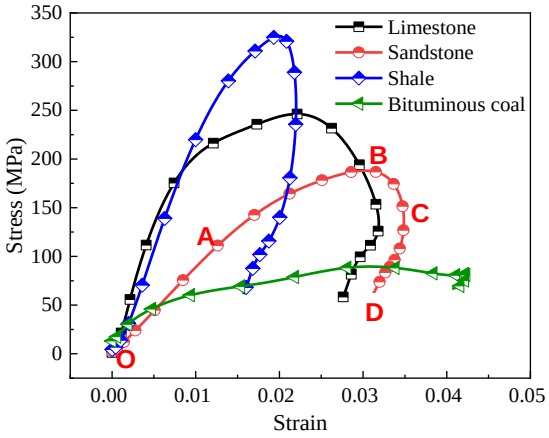

Fig. 4 Stress-strain curves of rocks and bituminous coal

indicates limestone has the strongest resistance to deformation during the elastic phase. The bituminous coal has the lowest elastic modulus of 8.29 GPa.

(3) Plastic deformation stage (BC). The stress and strain indicated a nonlinear relationship until reaching the compression strength. Point C represents the compression strength. The compression strength of the limestone, sandstone, shale, and bituminous coal is 48.33 MPa, 20.05 MPa, 77.98 MPa, and 15.96 MPa, respectively.

(4) Post-peak failure stage (CD). The stress-strain curve of the limestone and bituminous coal showed a sudden downtrend. However, the sandstone showed a downward trend with oscillations, which indicates that it didn't rupture immediately after reaching compression strength. And there was no obvious post-peak failure stage in shale, which indicates that it was destroyed rapidly after reaching the peak stress. At this stage, cracks developed greatly in rocks and the micro-cracks grew into large macro-cracks.

In a word, unlike rocks, the bituminous coal had an obvious pore compaction stage. And the static compression strength and elastic modulus were much smaller than that of rocks. Because the texture of bituminous coal is loose and there are more abundant pores and cracks.

3.2 Response of coals to low-speed dynamic loading

3.2.1 Dynamic stress-strain curves of coals

Fig.4 gives typical dynamic stress-strain curves (0.06 MPa air pressure for example). Each dynamic stress-strain curve can be divided into four stages, taking sandstone as an example.

(1) Linear elastic stage (OA). The curves showed a sharper increase at the initial stage. The modulus of elasticity of the limestone, sandstone, shale, and bituminous coal is 42.80 GPa, 14.29 GPa, 21.48 GPa, and 9.32 GPa, respectively, which shows that limestone has the strongest resistance to elastic deformation, while the bituminous coal has the lowest resistance to elastic deformation.

(2) Nonlinear stage (AB). The dynamic compression strength of the rocks increased significantly and showed a distinct strain hardening effect due to significant plastic deformation. The stress at point B showed the dynamic compression strength. The dynamic compression strength of limestone, sandstone, shale, and bituminous coal is 185.9 MPa, 151.7 MPa, 252.7 MPa, and 89.9 MPa, which are all much higher than their static mechanical strengths.

(3) Unloading stage (BC). Point C represents the ultimate strain of the rocks and coal, that is the maximum deformation of the specimen under dynamic loading. Under the same dynamic loading, the ultimate strain of shale is the smallest, indicating that it has the strongest resistance to deformation, while the bituminous coal has the largest ultimate strain and weak resistance to deformation.

(4) Curve rebound stage (CD). The strain was reduced because the stored strain energy was released quickly, which resulted in a significantly closed-loop behind the peak of the dynamic stress-strain curve. The strain at this stage showed an obvious hysteretic phenomenon, which indicated that the samples still had partial compression resistance. Besides, at point D, the rock was broken and the rebound stopped.

Due to the loose and multi-fracture characteristics of coal, the dynamic compression strength of bituminous coal was much smaller than those of rocks. Its ultimate strain is greater than the rocks, which indicates that the resistance to deformation is the weakest. The stress-strain curve of the bituminous coal in the rebound stage was short, which shows that the residual compression resistance of the bituminous coal is weak after the destruction.

Fig. 5 shows the dynamic stress-strain curves of three rocks and bituminous coal under different dynamic loading (characterized by air pressure shown in the figure). The dynamic compression strength of the rocks increases with the increase of the dynamic loading. However, the elastic modulus of limestone and sandstone is the largest at 0.06 MPa, which shows that the two rocks have the strongest resistance to elastic deformation at this loading. However, the elastic modulus of shale is not sensitive to dynamic loading. Similarly, the ultimate strain of rocks is the smallest at 0.06 MPa, indicating that it has the strongest resistance to deformation at this loading. The ultimate strain of bituminous coal increases with increasing dynamic loading. Due to the heterogeneity of bituminous coal, there is no obvious regularity of elastic modulus and dynamic compression strength.

3.2.2 Dynamic impact parameters

As shown in Table 2, the dynamic compression strength of the rocks and bituminous coal is much greater than their static compression strength. The strain rate and dynamic compression strength of rocks increased with the increase of dynamic loading. Compared with static compression strength, the dynamic compression strength of limestone at 0.05 MPa, 0.06 MPa, and 0.08 MPa increased by 226.91%, 284.85%, and 409.00%, respectively. The dynamic compression strength of sandstone increased by 496.01%, 656.61%, and 836.16%, respectively. The dynamic compression strength of shale increased by 152.63%, 224.44%, and 318.06%, respectively. The results show that the lower the static compression strength of rocks, the faster the dynamic compression strength increases. The ultimate strain is the smallest at 0.06 MPa, and similar at 0.05 MPa

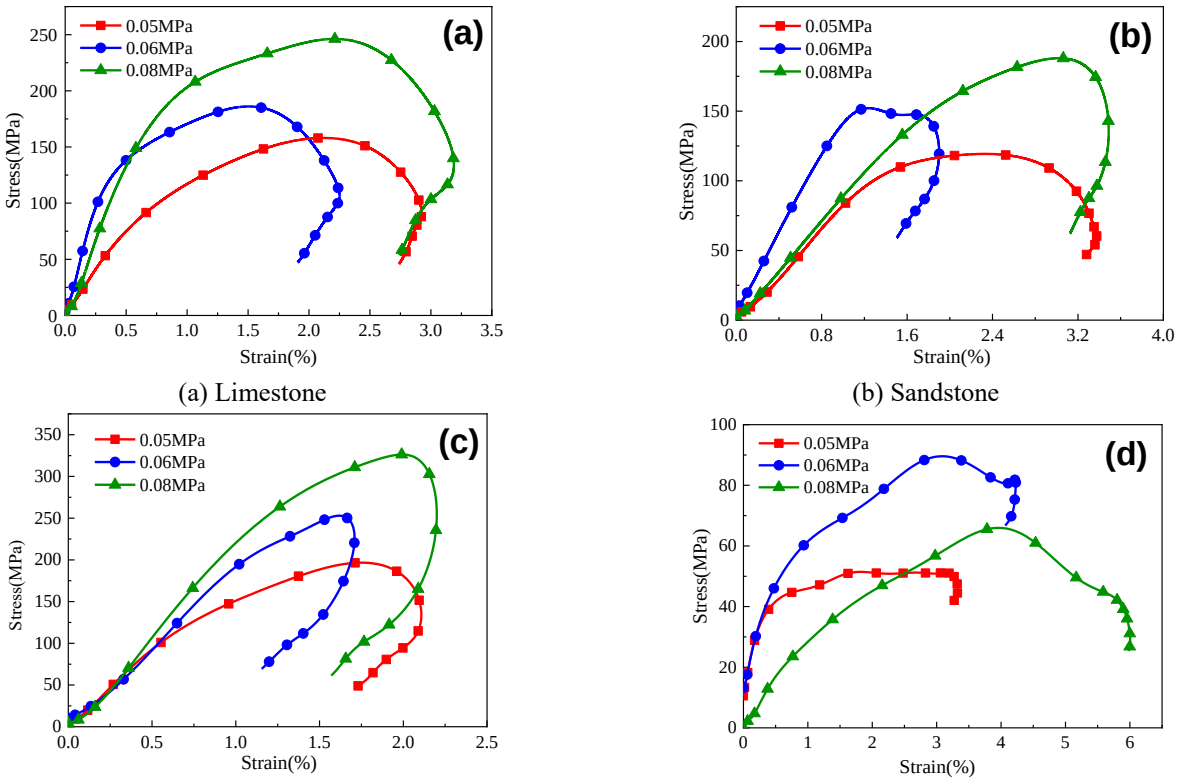

(a) Limestone (b) Sandstone

(c) Shale (d) Bituminous coal

Fig. 5 Stress-strain curves of rock cores under different air pressure

Table 2 Experimental results of dynamic mechanical parameters

Rock Code	Air pressure /MPa	Striker velocity /m.s^{-1}	Strain rate/s^{-1}	Compression strength /MPa	Ultimate strain	Elasticity modulus /GPa	DIF
LS1	0.05	1.64	200.86	157.8	0.029	15.32	3.27
LS2	0.06	1.91	237.29	185.9	0.023	42.80	3.85
LS3	0.08	2.44	289.82	246.1	0.032	29.74	5.09
SS1	0.05	1.56	167.31	119.5	0.034	8.92	5.96
SS2	0.06	1.89	232.89	151.7	0.019	14.29	7.57
SS3	0.08	2.43	289.82	187.7	0.035	8.93	9.36
SH1	0.05	1.58	182.22	196.6	0.021	19.46	2.52
SH2	0.06	2.00	195.16	252.7	0.017	21.48	3.24
SH3	0.08	2.42	240.65	325.7	0.022	25.17	4.18
BT1	0.05	1.50	217.42	51.6	0.033	9.27	3.23
BT2	0.06	1.97	317.97	89.9	0.042	9.32	5.63
BT3	0.08	2.54	424.05	65.94	0.060	2.03	4.13

*LS-limestone; SS-sandstone; SH-shale; BT-bituminous coal

and 0.08 MPa, which indicates that the resistance to deformation is the strongest at 0.06 MPa. The elastic modulus has no obvious relationship with the increase of dynamic loading.

However, the dynamic compression strength of the bituminous coal has no obvious relationship with the increase of dynamic loading. Because of the physical and chemical heterogeneity of coal (Botto *et al*. 1994, Li *et al.* 2012), the development degree of internal cracks of different coal cores are different, so the dynamic compression strength is greatly affected by coal cores. In addition, the strain rate and ultimate strain of bituminous coal gradually increase with the increase of dynamic loading. Crack has sufficient time to grow and develop under a slow and static loading, so the material could fail at lower loading. On the contrary, crack does not have enough time to grow under a high strain rate, so higher dynamic strength can be achieved before the material fails.

Fig. 6 shows a relationship between the dynamic compression strength and the strain rate. The dynamic

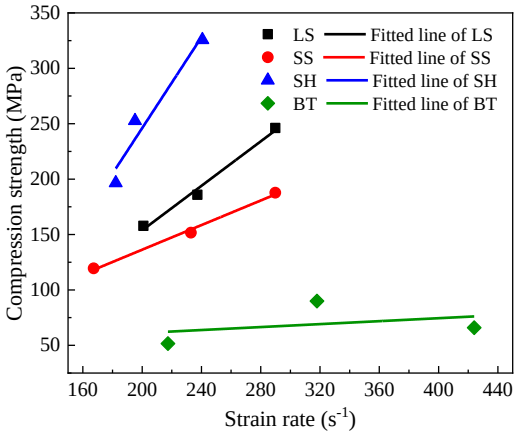

Fig. 6 The relationship between compression strength and strain rate

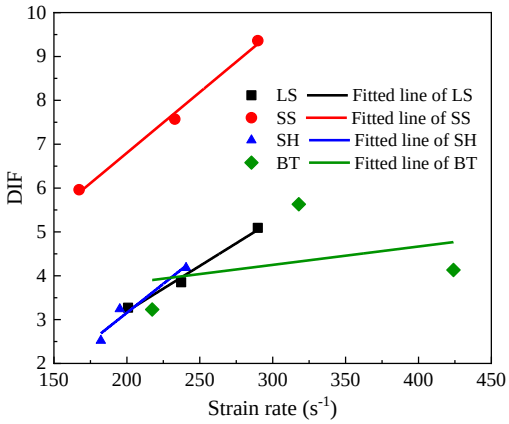

Fig. 7 The relationship between DIF and strain rate

compression strength of rocks and bituminous coal increased linearly with increasing strain rate. The dependence of dynamic compression strength on strain rate was fitted by Eqs. (8)-(11)

$$\text{LS: } f_{LS}=1.00\varepsilon-46.88 \quad 200\ s^{-1} \le \varepsilon \le 290 s^{-1} \quad (R^2=0.98948) \tag{8}$$

$$\text{SS: } f_{SS}=0.56\varepsilon+25.30 \quad 167\ s^{-1} \le \varepsilon \le 290 s^{-1} \quad (R^2=0.99469) \tag{9}$$

$$\text{SH: } f_{SH}=2.05\varepsilon-164.20 \quad 182 s^{-1} \le \varepsilon \le 240 s^{-1} \quad (R^2=0.94545) \tag{10}$$

$$\text{BT: } f_{BT}=0.0667\varepsilon+47.82 \quad 217 s^{-1} \le \varepsilon \le 424 s^{-1} \quad (R^2=0.12684) \tag{11}$$

Where, f and ε are dynamic compression strength and strain rate, respectively.

The dynamic compression strength of rocks increases linearly with increasing strain rate and the fitting degree is greater than 94%. However, the fitting degree of the bituminous coal is only 13%, indicating that the dynamic compression strength of the bituminous coal has no obvious regularity with the increase of strain rate due to the heterogeneity of coal. For rocks, the higher the static compression strength, the faster the rate of increase of the dynamic compression strength and the higher the strain rate sensitivity. The dynamic compression strength of shale is greater than that of limestone and sandstone.

The higher the strain rates, the bigger the dynamic compression strength, which can be explained by fracture mechanics concepts (John *et al.* 1987, Zhang *et al.* 2010). According to the Griffith theory with the concept of sub-critical crack growth, failure occurs when the deformation of the materials exceeds its critical deformation (Erarslan and Williams 2012). If the loading is applied slowly, the cracks have sufficient time to grow. Therefore, the rocks fail at lower loading and show lower compression strength. When the loading rate is fast enough, there is little time for the growth of the subcritical flaws, and a higher dynamic compression strength can be achieved before the failure of the rock. As discussed by (Zhou *et al*. 2010), the number of pre-peak cracks is reduced at high-rate loading. This applies before the unloading phase. For the unloading stage, the cracks increase rapidly at a high strain rate and absorb more energy, which is characterized by higher dynamic compression strength (Reinhardt and Cornelissen 1986).

Fig. 7 illustrates the relationship between dynamic increase factor (DIF) and strain rate. Dynamic increase factor (DIF), the ratio of dynamic strength to static strength, has been widely used to measure the effect of strain rate on the strength of rocks (Li and Meng 2003, Chakraborty *et al.* 2016). The DIF of the rocks increases linearly with the increase of the strain rate, which is similar to the research result of (Ren *et al.* 2015). The fitting formulas of rocks and bituminous coal were as follows.

$$\text{LS: } DIF_{LS}=0.021\varepsilon-0.948 \quad 200\ s^{-1} \le \varepsilon \le 290 s^{-1} \quad (R^2=0.98958) \tag{12}$$

$$\text{SS: } DIF_{SS}=0.277\varepsilon+1.265 \quad 167\ s^{-1} \le \varepsilon \le 290 s^{-1} \quad (R^2=0.99493) \tag{13}$$

$$\text{SH: } DIF_{SH}=0.026\varepsilon-2.121 \quad 182 s^{-1} \le \varepsilon \le 240 s^{-1} \quad (R^2=0.94587) \tag{14}$$

$$\text{BT: } DIF_{BT}=0.004\varepsilon+2.991 \quad 217 s^{-1} \le \varepsilon \le 424 s^{-1} \quad (R^2=0.12728) \tag{15}$$

Similar to the dynamic compression strength, the DIF of rocks increases linearly with the increase of strain rate, while the DIF of bituminous coal has no obvious linear relationship (R^2=0.12728) with the increase of strain rate due to the heterogeneity of coal. In addition, the DIF growth rates of the three rocks are similar, as confirmed by the slope in the formula, which indicates that the strain rate has little effect on the DIF growth rate of the three rocks.

3.2.3 Absorbed energy and its relationship with the strain rate

In the SPHB experiments, involved energies include impact kinetic energy (W_I), transmitted energy (W_T), and reflected energy (W_R). Besides, vaseline is applied to both ends of the rocks as “lubricant”, so energy loss due to frictional force between the bar and the rocks is negligible. Thus, the absorbed energy(W_A) contributing to rock failure can be calculated by

$$W_A = W_I - W_R - W_T \tag{16}$$

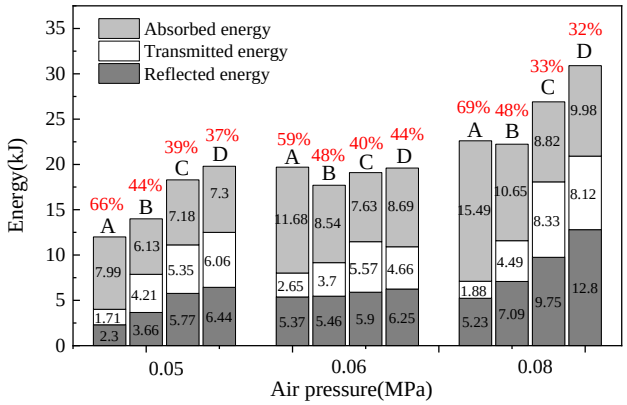

Fig. 8 Relationship between energy and dynamic loading. A- the bituminous coal; B-the sandstone; C-the shale; D- the limestone

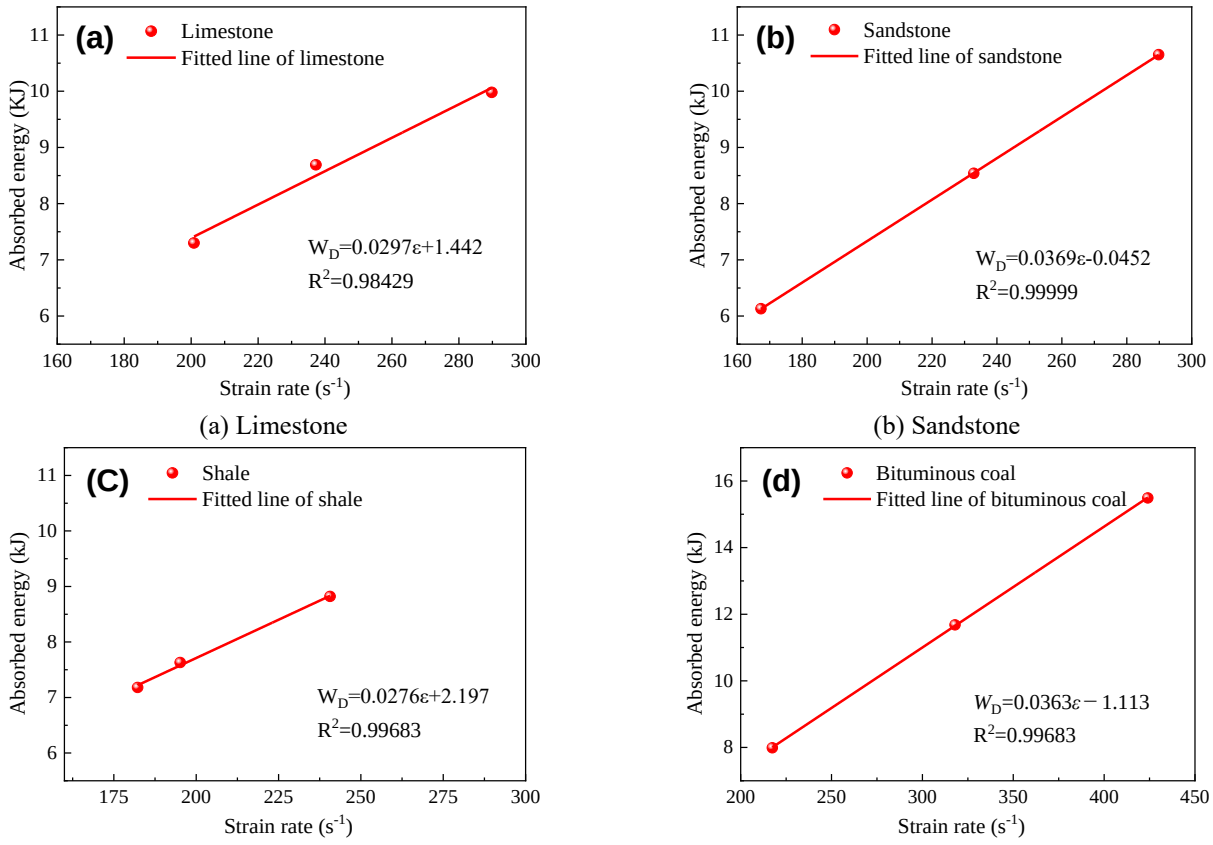

(a) Limestone (b) Sandstone

(c) Shale (d) Bituminous coal

Fig. 9 Relationship between strain rate and absorbed energy

The rock damage level is related to the energy of absorbed stress wave, which can be expressed by energy absorbed rate N

$$N = \frac{W_D}{W_I} \times 100\% \tag{17}$$

Fig. 8 shows the relationship between the energy and the dynamic loading. The total energy increased with the increase of dynamic loading as expected, which is due to the growth of impact kinetic energy of the striker bar. Meanwhile, the absorbed energy, which directly contributes to the failure of rocks, also increased with the dynamic loading. The ratio of the absorbed energy to the total energy of bituminous coal is greater than that of rocks because there are more internal cracks in bituminous coal, and crack propagation needs to absorb more energy. Compared with low strain rate, the growth of pre-peak crack will be reduced under high strain rate, while for the post-peak unloading stage, the growth of crack absorbs more energy, which is manifested as the higher dynamic compressive strength.

Fig. 9 shows a relationship between the absorbed energy

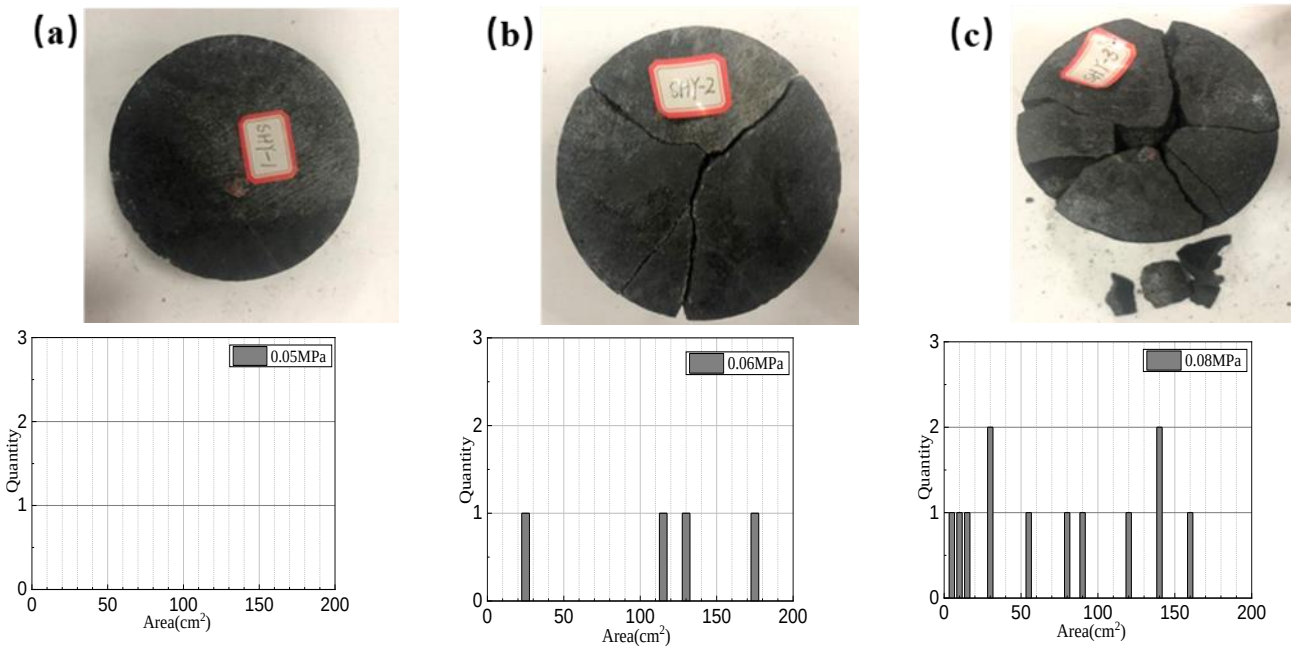

(a) 0.05 MPa (b) 0.06 MPa (c) 0.08 MPa

Fig. 10 Crushed limestone under different dynamic loading.

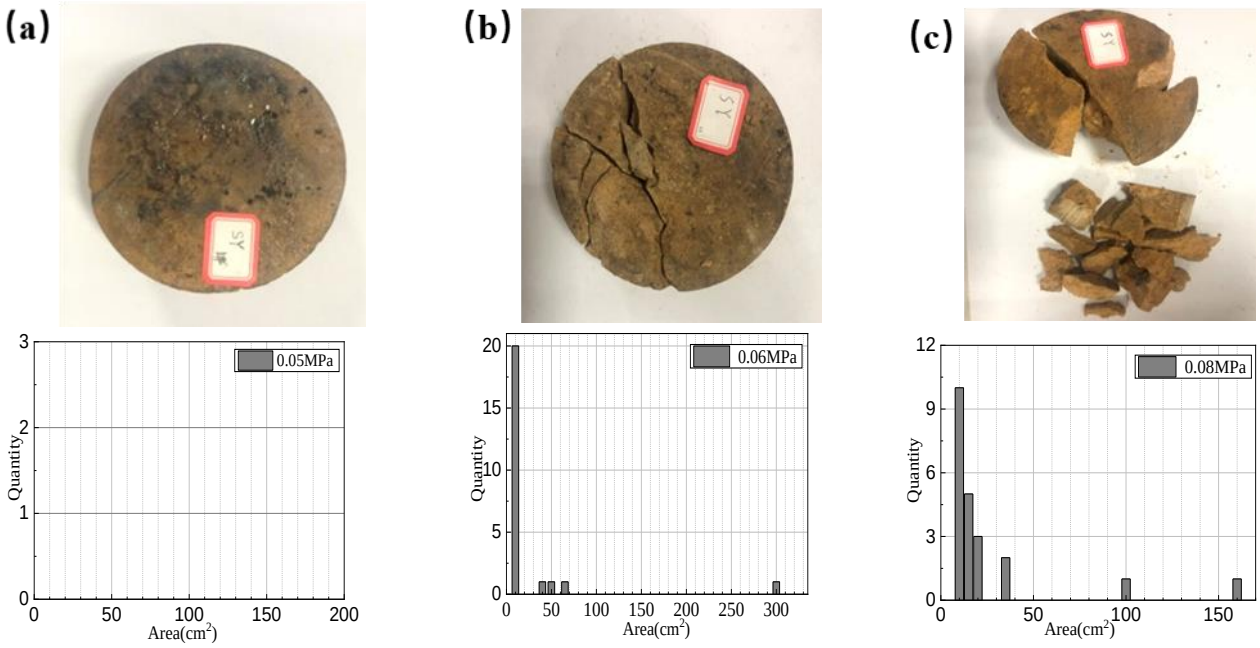

(a) 0.05 MPa (b) 0.06 MPa (c) 0.08 MPa

Fig. 11 Crushed sandstone under different dynamic loading.

and the strain rate. The absorbed energy (W_D) of the rock cores are fitted by W_D=aε+b, where, a and b are fitting parameters, ε is the strain rate. The absorbed energy directly affects the failure morphology of rocks (Hokka *et al*. 2016). In our experiments, the absorbed energy increased linearly with increasing strain rate, which was also found by (Li *et al.* 2005). The slope of the curves represents the strain rate sensitivity of the sample, which means that the greater the slope, the greater the effect of the absorbed energy on the strain rate. The sandstone and the bituminous coal have higher strain rate sensitivity than those of limestone and shale. Because the sandstone and the bituminous coal have lower static strength and weaker resistance to deformation, the cracks generated by cores are more abundant at the same dynamic loading, the energy will be absorbed more.

Figs. 10-13 shows the crushed morphology of rocks and bituminous coal under different dynamic loading. Photos above are crushed rock and coal cores, and bar charts below show their fragment size distribution. Failure of the rocks or coals mainly occurred at the unloading stage, which would

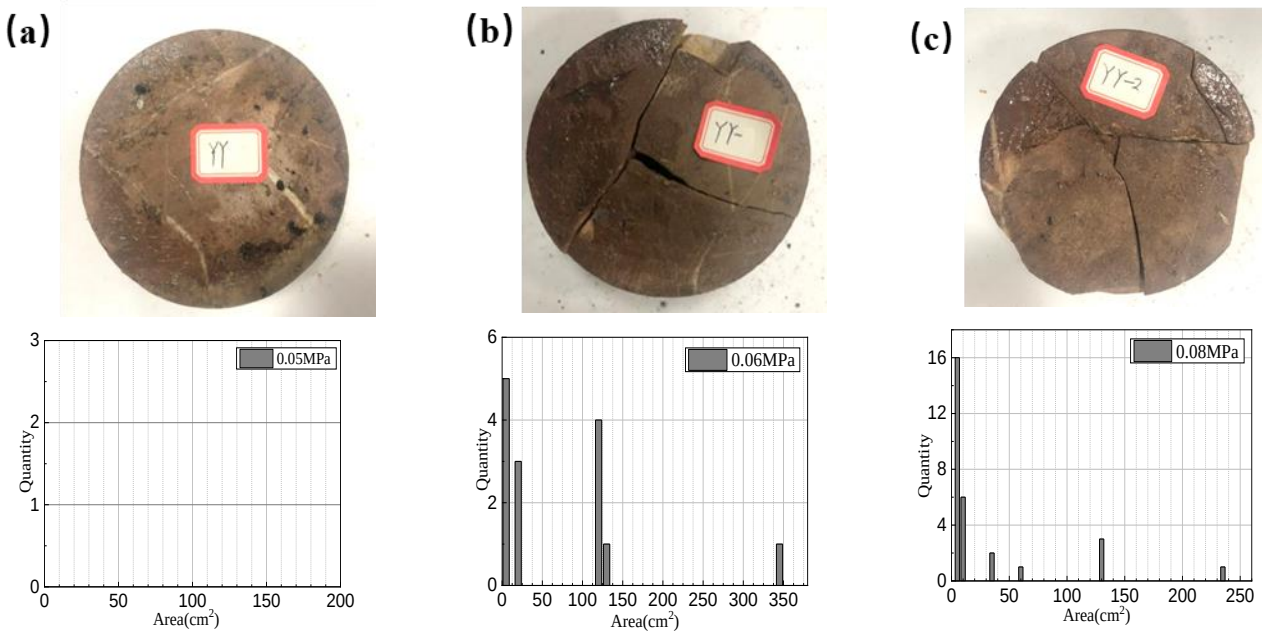

(a) 0.05 MPa (b) 0.06 MPa (c) 0.08 MPa

Fig. 12 Crushed shale under different dynamic loading

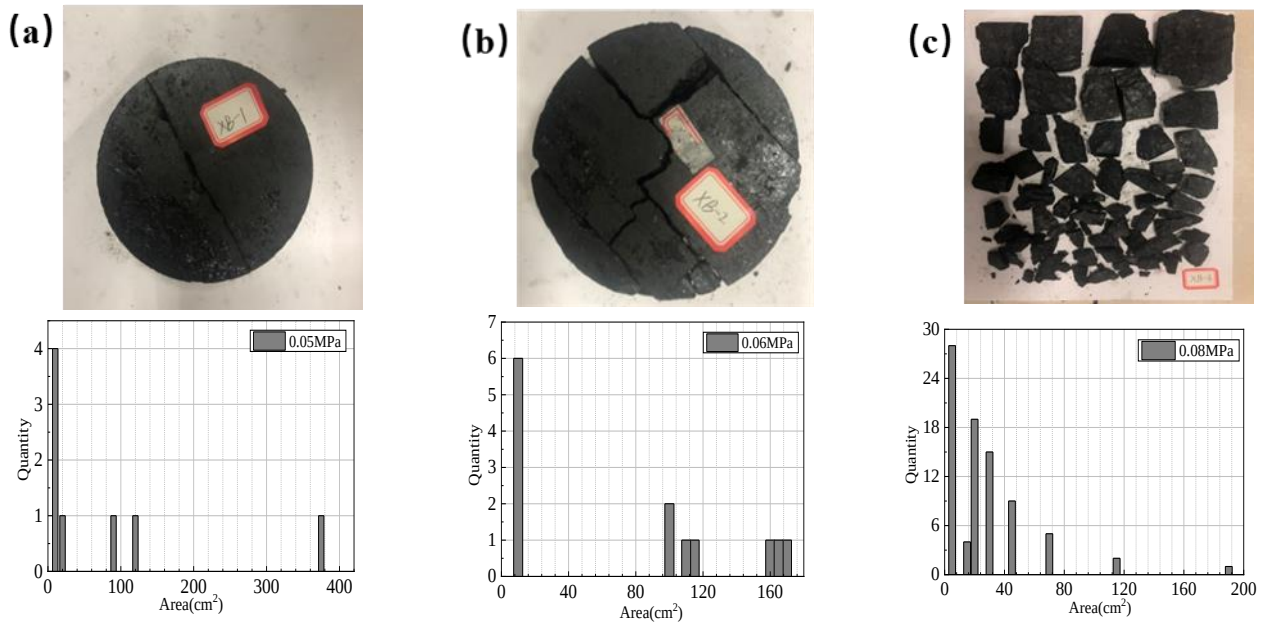

(a) 0.05 MPa (b) 0.06 MPa (c) 0.08 MPa

Fig. 13 Crushed bituminous coal under different dynamic loading.

lead to crack propagation as a result of absorbing energy. As the dynamic loading increased, the rocks and coal ruptured more seriously due to the more absorbed energy. According to Fig. 9, when the dynamic loading increased, absorbed energy rose and more fragments of ruptured rocks and coal can be expected (Li *et al.* 2005). Absorbed energy should be closely related to the content of micropores. As the pressure increases, the content of micropores in the rock will increase, which is a key factor for increasing absorbed energy.

Fragment area distributions were s counted by the grid method (Zhu *et al.* 2013). Small-scale fragments are an important basis for measuring the level of rock damage(Hogan *et al.* 2012). For different kinds of rocks, their degree of rupture is determined by the static compression strength. Since the static strength of sandstone is the lowest compared to limestone and shale, there was a larger number of small-scale fragments. Moreover, the static compression strength of the bituminous coal is lower than that of rocks, so the number of small-scale fragments was the largest.

Generally speaking, the degree of heterogeneity of coal

is greater than that of rock, and the original cracks are relatively more. Local deformation and failure of coal are easy to occur in the compression process, leading to the loss of the bearing capacity, which is manifested by lower compressive strength and smaller fragment size. On the contrary, the rock is relatively dense with a low degree of heterogeneity, which results in relatively few cracks and strong anti-deformation ability. The failure mode of rock is larger crack penetration and larger fragment size.

4. Conclusions

At the same dynamic loading, the dynamic compression strength of the shale is greater than that of limestone and sandstone. Moreover, with the increase of the dynamic loading, the dynamic compression strength of the rocks increases gradually, but the bituminous coal is irregular due to the characteristics of multi-fracture and heterogeneity.

The dynamic compression strength of the rocks and bituminous coal is both much greater than their static compression strength. The dynamic compression strength and dynamic increase factor of the rocks both increase linearly with the increase of the strain rate, while those of the bituminous coal have no obvious regularity. The higher the static compression strength of rocks, the faster the rate of increase of the dynamic compression strength and the higher the strain rate sensitivity. However, rocks of different strengths have no significant effect on the growth rate of the dynamic increase factor.

The absorbed energy increases linearly with an increase of strain rate. The ratio of absorbed energy to the total energy of bituminous coal is greater than that of rocks because there are more internal cracks in bituminous coal, and crack propagation needs to absorb more energy. For the same kind of rocks and bituminous coal, the higher the dynamic loading, the greater the degree of rupture. For different kinds of rocks, the lower the static strength of the rocks, the greater the degree of failure at the same dynamic pressure. The static compassion strength of the bituminous coal is lower than that of rocks, so the number of small-scale fragments was the largest after bituminous coal rupture.

Acknowledgments

Financial support provided by the National Natural Science Foundation of China (NSFC) (Grant Number: 51874293) and National Science and Technology Major Project (Grant Number: 2020YFA0711803) for this research is gratefully acknowledged.

References

Abrams, D.A. (1917), "Effect of rate of application of load on the compressive strength of concrete", *ASTM J*, **17**(2), 364-377.

Bieniawski, Z.T. (1968), "Fracture dynamics of rock", *Fract. Mech.*, **4**(4), 415-430. https://doi.org/10.1007/BF00186807.

Blanton, T.L. (1981), "Effect of strain rates from 10 -2 to 10 sec -1 in triaxial compression tests on three rocks", *Int. J. Rock. Mech. Min.*, **18**(1), 47-62. https://doi.org/10.1016/0148-9062(81)90265-5.

Botto, R.E., Cody, G.D., Kirz, J., Ade, H., Behal, S. and Disko, M. (1994), "Selective chemical mapping of coal microheterogeneity by scanning transmission x-ray microscopy", *Energ. Fuel.*, **8**(1), 151-154. https://doi.org/10.1021/ef00043a026.

Brown, E.T. and Hoek, E. (1978), "Trends in relationships between measured in-situ stresses and depth", *Int. J. Rock. Mech. Min.*, **15**(4), 211-215. https://doi.org/10.1016/0148-9062(78)91227-5.

Cai, M. (2008), "Influence of intermediate principal stress on rock fracturing and strength near excavation boundaries—Insight from numerical modeling", *Int. J. Rock. Mech. Min.*, **45**(5), 763-772. https://doi.org/10.1016/j.ijrmms.2007.07.026.

Chakraborty, T., Mishra, S., Loukus, J., Halonen, B. and Bekkala, B. (2016), "Characterization of three Himalayan rocks using a split Hopkinson pressure bar", *Int. J. Rock. Mech. Min.*, **85**, 112-118. https://doi.org/10.1016/j.ijrmms.2016.03.005.

Chen, S., Yin, D. and Jiang, N. (2019), "Simulation study on effects of loading rate on uniaxial compression failure of composite rock-coal layer", *Geomech.Eng.*, **17**(4), 333-342. https://doi.org/10.12989/gae.2019.17.4.333.

Cho, S.H., Ogata, Y. and Kaneko, K. (2003), "Strain-rate dependency of the dynamic tensile strength of rock", *Int. J. Rock. Mech. Min.*, **40**(5), 763-777. https://doi.org/10.1016/S1365-1609(03)00072-8.

Crespo, M., Río, G.D. and Rodríguez, J. (2017), "Failure of SLS polyamide 12 notched samples at high loading rates", *Theor. Appl. Fract. Mech.*, **92**, 233-239. https://doi.org/10.1016/j.tafmec.2017.08.008.

Davies, E.D.H. and Hunter, S.C. (1963), "The dynamic compression testing of solids by the method of the split Hopkinson pressure bar", *Mech. Phys. Solids*, **11**(3), 155-179. https://doi.org/10.1016/0022-5096(63)90050-4.

Demirdag, S., Tufekci, K., Kayacan, R., Yavuz, H. and Altindag, R. (2010), "Dynamic mechanical behavior of some carbonate rocks", *Int. J. Rock. Mech. Min.*, **47**(2), 307-312. https://doi.org/10.1016/ j.ijrmms.2009.12.003.

Erarslan, N. and Williams, D.J. (2012), "The damage mechanism of rock fatigue and its relationship to the fracture toughness of rocks", *Int. J. Rock. Mech. Min.*, **56**, 15-26. https://doi.org/10.1016/ j.ijrmms.2012.07.015..

Feng, J., Wang, E. and Shen, R. (2016), "Investigation on energy dissipation and its mechanism of coal under dynamic loads", *Geomech. Eng.*, **11**(5), 657-670. https://doi.org/10.12989/gae.2016.11.5.657.

Field, J.E., Walley, S.M., Proud, W.G., Goldrein, H.T. and Siviour, C.R. (2004), "Review of experimental techniques for high rate deformation and shock studies", *Int. J. Impact Eng.*, **30**(7), 725-775. https://doi.org/10.1016/j.ijimpeng.2004.03.005.

Frew, D.J., Forrestal, M.J. and Chen, W. (2001), "A split Hopkinson pressure bar technique to determine compressive stress-strain data for rock materials", *Exp. Mech.*, **41**(1), 40-46. https://doi.org/10.1007/ BF02323102.

Gama, B.A., Lopatnikov, S.L. and Gillespie, J.W. (2004), "Hopkinson bar experimental technique: A critical review", *Appl. Mech.Rev.*, **57**(4), 223. https://doi.org/10.1115/1.1704626.

He, M.C., Sousa, L.R.E., Miranda, T. and Zhu, G.L. (2015), "Rockburst laboratory tests database — Application of data mining techniques", *Eng. Geol.*, **185**, 116-130. https://doi.org/10.1016/j.enggeo.2014.12.008.

Hogan, J.D., Rogers, R.J., Spray, J.G. and Boonsue, S. (2012), "Dynamic fragmentation of granite for impact energies of 6–

28 J", *Eng. Fract. Mech.*, **79**, 103-125. https://doi.org/10.1016/j.engfracmech.2011.10.006.

Hokka, M., Black, J., Tkalich, D., Fourmeau, M., Kane, A., Hoang, N.H., Li, C.C. and Chen, W.W. (2016), "Effects of strain rate and confining pressure on the compressive behavior of Kuru granite", *Int. J. Impact Eng.*, **91**, 183-193. https://doi.org/10.1016/j.ijimpeng.2016.01.010.

John, R., Shah, S.P. and Jeng, Y.S. (1987), "A fracture mechanics model to predict the rate sensitivity of mode I fracture of concrete", *Cement Concr. Res.*, **17**(2), 249-262. https://doi.org/10.1016/0008-8846(87)90108-6.

Kim, E., Garcia, A. and Changani, H. (2018), "Fragmentation and energy absorption characteristics of Red, Berea and Buff sandstones based on different loading rates and water contents", *Geomech. Eng.*, **14**(2), 151-159. https://doi.org/10.12989/gae.2018.14.2.000.

Kolsky, H. (1964), "Stress waves in solids", *J. Sound Vib.*, **1**(1), 88-110. https://doi.org/10.1016/0022-460X(64)90008-2.

Li, J.C., Ma, G.W. and Zhou, Y.X. (2012), "Analytical Study of Underground Explosion-Induced Ground Motion", *Rock. Mech. Rock. Eng.*, **45**(6), 1037-1046. https://doi.org/ 10.1007/s00603-011-0200-3.

Li, Q.M. and Meng, H. (2003), "About the dynamic strength enhancement of concrete-like materials in a split Hopkinson pressure bar test", *Int. J. Solids Struct.*, **40**(2), 343-360. https://doi.org/10.1016/S0020-7683(02)00526-7.

Li, S., Tang, D.Z., Xu, H. and Yang, Z. (2012), "Advanced characterization of physical properties of coals with different coal structures by nuclear magnetic resonance and X-ray computed tomography", *Comput. Geosci.*, **48**(48), 220-227. https://doi.org/10.1016/j.cageo.2012.01.004.

Li, X.B., Lok, T.S. and Zhao, J. (2005), "Dynamic characteristics of granite subjected to intermediate loading rate", *Rock. Mech. Rock. Eng.*, **38**(1), 21-39. https://doi.org/10.1007/s00603-004-0030-7.

Li, Y., Zhang, S. and Zhang, B. (2018), "Dilatation characteristics of the coals with outburst proneness under cyclic loading conditions and the relevant applications", *Geomech. Eng.*, **14**(5), 459-466. https://doi.org/ 10.12989/gae.2018.14.5.459.

Liu, H.Y., Roquete, M. and Kou, S.Q. (2004), "Characterization of rock heterogeneity and numerical verification", *Eng. Geol.*, **72**(1-2), 89-119. https://doi.org/10.1016/j.enggeo.2003.06.004.

Liu, K., Zhang, Q.B., Wu, G., Li, JC. and Zhao, J. (2019), "Dynamic mechanical and fracture behaviour of sandstone under multiaxial loads using a triaxial Hopkinson bar", *Rock. Mech. Rock. Eng.*, (52), 2175-2195. https://doi.org/10.1007/s00603-018-1691-y.

Liu, S. and Xu, J.Y. (2015), "Effect of strain rate on the dynamic compressive mechanical behaviors of rock material subjected to high temperatures", *Mech. Mater.*, **82**, 28-38. https://doi.org/10.1016/ j.mechmat.2014.12.006.

Liu, T., Lin, B. and Yang, W. (2017), "Impact of matrix–fracture interactions on coal permeability: Model development and analysis", *Fuel*, **207**, 522-532. https://doi.org/10.1016/j.fuel.2017.06.125.

Meng, Q., Zhang, M., Han, L., Pu, H. and Nie, T. (2016), "Effects of acoustic emission and energy evolution of rock specimens under the uniaxial cyclic loading and unloading compression", *Rock. Mech. Rock. Eng.*, **49**(10), 1-14. https://doi.org/ 10.1007/s00603-016-1077-y.

Read, R.S. (2004), "20 years of excavation response studies at AECL's Underground Research Laboratory", *Int. J. Rock. Mech. Min.*, **41**(8), 1251-1275. https://doi.org/10.1016/j.ijrmms.2004.09.012.

Reinhardt, B.H.W. and Cornelissen, H.A.W. (1986), "Tensile tests and failure analysis of concrete", *J. Struct. Eng.*, **112**, 2462-2477. https://doi.org/10.1061/(ASCE)0733-9445(1986)112:11(2462).

Ren, W., Xu, J., Liu, J. and Su, H. (2015), "Dynamic mechanical properties of geopolymer concrete after water immersion", *Ceram. Int.*, **41**(9), 11852-11860. https://doi.org/10.1016/j.ceramint.2015.05.154.

Tao, M., Ma, A., Cao, W., Li, X. and Gong, F. (2017), "Dynamic response of pre-stressed rock with a circular cavity subject to transient loading", *Int. J. Rock. Mech. Min.*, **99**, 1-8.
https://doi.org/ 10.1016/j.ijrmms.2017.09.003

Tarasov, B.G. (1990), "Simplified method for determining the extent to which strain rate affects the strength and energy capacity of rock fracture", *Sov.Min.Sci.*, **26**(4), 315-320. https://doi.org/10.1007/BF02506510.

Wang, J.A. and Park, H.D. (2001), "Comprehensive prediction of rockburst based on analysis of strain energy in rocks", *Tunn.Undergr. Sp.Tech.*, **16**(1), 49-57. https://doi.org/10.1016/S0886-7798(01)00030-X.

Wang, Q.Z., Li, W. and Song, X.L. (2006), "A Method for Testing Dynamic Tensile Strength and Elastic Modulus of Rock Materials Using SHPB", *Pure Appl. Geophys.*, **163**(5-6), 1091-1100. https://doi.org/ 10.1007/s00024-006-0056-8.

Wang, T., Song, Z. and Yang, J. (2019), "Experimental research on dynamic response of red sandstone soil under impact loads", *Geomech.Eng.*, **17**(4), 393-403. https://doi.org/10.12989/ gae.2019.17.4.393.

Wla, B., Jya, B., Peng, Y., Ming, C., Cza, B., Yi, L. and Li, J. (2012), "Dynamic response of rock mass induced by the transient release of in-situ stress", *Int. J. Rock. Mech. Min.*, **53**, 129-141. https://doi.org/ 10.1016/j.ijrmms.2012.05.001

Yaméogo, S., Corthésy, R. and Leite, M.H. (2013), "Influence of rock failure and damage on in situ stress measurements in brittle rock", *Int. J. Rock. Mech. Min.*, **61**, 118-129. https://doi.org/ 10.1016/j.ijrmms.2013.02.011.

Yao, W., Xu, Y. and Yu, C. (2017), "A dynamic punch-through shear method for determining dynamic Mode II fracture toughness of rocks", *Eng. Fract. Mech.*, **176**, 161-177. https://doi.org/10.1016/ j.engfracmech.2017.03.012.

Yavuz, H., Tufekci, K., Kayacan, R. and Cevizci, H. (2013), "Predicting the Dynamic Compressive Strength of Carbonate Rocks from Quasi-Static Properties", *Exp. Mech.*, **53**(3), 367-376. https://doi.org/ 10.1007/s11340-012-9648-7.

Yilmaz, O. and Unlu, T. (2013), "Three-dimensional numerical rock damage analysis under blasting load", *Tunn. Under. Sp. Tech.*, **38**, 266-278. https://doi.org/ 10.1016/j.tust.2013.07.007.

Zhang, X.X., Yu, R.C., Ruiz, G. Tarifa, M. and Camara, M.A. (2010), "Effect of loading rate on crack velocities in HSC", *Int. J. Impact Eng.*, **37**(4), 359-370. https://doi.org/10.1016/j.ijimpeng.2009.10.002.

Zhou, Z., Li, X., Ye, Z. and Liu, K. (2010), "Obtaining constitutive relationship for rate-dependent rock in SHPB tests", *Rock. Mech. Rock. Eng.*, **43**(6), 697-706. https://doi.org/10.1007/s00603-010-0096-3.

Zhu, C.J., Lin, B.Q., Jiang, B.Y., Liu, Q. and Sun, Y.M. (2013), "Multiphase destructive effects of shock wave resulting from coal mine gas explosion", *J. China. U. Min. Techno.*, **42**(5), 718-724+730. https://doi.org/ 10.13247/j.cnki.jcumt.2013.05.003.

Zhu, J.B., Liao, Z.Y. and Tang, C.A. (2016), "Numerical SHPB tests of rocks under combined static and dynamic loading conditions with application to dynamic behavior of rocks Under in situ stresses", *Rock. Mech. Rock. Eng.*, **49**(10), 1-12. https://doi.org/ 10.1016/j.ijimpeng.2012.04.002.

CC